UNCLASSIFIED

SAND2013-9308P

Technical Memorandum

SC-TM-70-418
May 1970

AN EXPERIMENTAL MEASUREMENT OF THE TOTAL ELECTRON CONTENT OF THE IONOSPHERE (U)

E. L. Whitlow
Vela Technology Division

R. D. Jones
Satellite Systems Division

Sponsored by
The Advanced Research Projects Agency

SANDIA LABORATORIES

OPERATED FOR THE UNITED STATES ATOMIC ENERGY COMMISSION BY SANDIA CORPORATION ALBUQUERQUE, NEW MEXICO, LIVERMORE, CALIFORNIA

Issued by Sandia Corporation,
a prime contractor to the
United States Atomic Energy Commission

SC-TN-70-418

AN EXPERIMENTAL MEASUREMENT OF THE TOTAL ELECTRON CONTENT OF THE IONOSPHERE

E. L. Whitlow
Vela Technology Division

R. D. Jones
Satellite Systems Division

Sandia Laboratories, Albuquerque

May 1970

Sponsored by the Advanced Research Projects Agency

ABSTRACT

Variation of the total electron content of the ionosphere with time has been determined by measurements of group velocities of signals propagated over a Vela satellite-earth path. By combining total electron content with ionizing component measurements, the primary mission of Vela can be extended to include studies of a variety of phenomena connected with effects of solar radiation on the ionosphere. In particular, it appears that the Vela satellite can provide high time resolution measurements on erratic variations associated with enhanced geomagnetic activity, particle precipitation, and other atmospheric disturbances.

ACKNOWLEDGMENTS

The authors wish to acknowledge the assistance of the Stanford Research Institute Staff, particularly Mr. Lambert Dolphin, in designing and operating the transmitters used in this experiment. The cooperation of Prof. Allen M. Peterson of Stanford University and Mr. W. C. Myre of Sandia Laboratories in arranging for SRI participation in the experiment is also appreciated.

TABLE OF CONTENTS

AN EXPERIMENTAL MEASUREMENT OF THE TOTAL ELECTRON CONTENT OF THE IONOSPHERE

I. INTRODUCTION

This report is concerned with the determination of the time variation in total electron content of the ionosphere by measuring the differential delay in the arrival of two quasi-monochromatic signals at a Vela satellite (nominal 10^5 km propagation path length). The measurement was made by use of satellite surveillance receivers not primarily intended for dispersion studies. The maximum columnar electron content was found to be in the neighborhood of 4×10^{17} electrons m^{-2}, a value not inconsistent with values determined by more conventional techniques. Accuracy of the measurements is estimated to be within $\pm 2 \times 10^{16}$ electrons m^{-2}.

By combining dispersion studies with studies of ionizing radiation from the sun, the primary mission of Vela can be extended to include studies of a variety of phenomena connected with the effects of solar radiation on the ionosphere. Dispersion measurements can be analyzed to provide information on the relation between production and loss of electrons in the F region of the ionosphere and the specific ionizing component responsible. More pragmatically, it appears that the Vela satellite can be used to provide information with high time resolution on erratic variations in the total electron content associated with enhanced geomagnetic activity, particle precipitation, and atmospheric disturbances.

The use of satellite radio beacons in the study of the ionosphere has become well established over the past several years. Dispersion measurements made over propagation paths between satellite radio beacons and receivers on the ground have been used extensively to determine the total, or columnar, electron content, i.e., the integrated electron content of the ionosphere over the propagation path.[1,2] In principle, there is no reason why measurements cannot be made with the use of signal sources on the ground and satellite-borne receivers. This

arrangement has not been used because replacing fairly simple beacons with complex receiving equipment is impractical for satellite applications. However, the receiving equipment can be considerably simplified if the dispersion measurement is carried out in the time domain rather than in the frequency domain.

During the late 1940's, with the ascendency of radio astronomy, observers noted variations in the apparent positions of radio stars.[3] These variations were attributed to refraction effects connected with the total ionization of the ionosphere. In fact, estimates were made of the total ionization of the F region, including the part above the maximum of ionization, from observations of the magnitude of the variation. The theory of ionospheric refraction had been published much earlier in the classical papers by Taylor and Hulburt,[4] and by Breit and Tuve.[5]

Since the early days of radar astronomy, the observed slow fading of moon echoes was attributed to rotation of the plane of polarization of the radio waves as they pass through the ionosphere (the Faraday effect[6]). Estimates of the integrated electron content of the ionosphere were obtained from measurements of the angular rotation of the plane of polarization of lunar echoes.[7,8] Studies of the total ionospheric electron content by observation of the Faraday effect on satellite signals began shortly after the launching of the first satellite in 1958.[9] At the same time, it was recognized that information on ionospheric electron content could also be obtained by measurements of the Doppler shift of satellite signals.[10,11] If there were no ionosphere, the Doppler shift in the frequency, observed on the ground, of signals transmitted from a satellite would be determined solely by the component of the velocity of the satellite in the direction of the straight line between the satellite and the receiver. Presence of the ionosphere modifies this Doppler shift since refraction causes a deviation from a straight-line propagation path.

It follows, then, that if the propagation path is distorted by the ionosphere, inferences on the ionospheric electron content can also be drawn by measuring the time interval for a signal to pass over the distorted path and by comparing this interval with the time required for a signal to propagate over the straight-line path. Such a procedure would require a knowledge of the satellite orbit elements to

a much higher degree of accuracy than one is ever likely to possess. However, when signals of two different frequencies can be transmitted simultaneously, it should be possible to ascertain the effect of the ionosphere by simply measuring the difference in arrival time of the two signals of different frequencies. Use of this technique has not been reported in the literature. It is, essentially, the time-domain analog of the two-beacon Doppler technique, in which ionospheric information is extracted from simultaneous measurements of the variation in frequency of two phase-coherent CW emissions. Either method obviates the need to know orbital data to an impossibly high order of precision.

In order to simplify the analysis which follows, a static ionosphere is assumed and the high-frequency approximation for the refractive index of the ionosphere is used. Effects of electron collisions and of the geomagnetic field have been neglected. Additional simplification is achieved by assuming a flat earth geometry. Finally, the "group velocity" is regarded as the velocity with which the modulation envelope travels, i.e., the propagation velocity of the energy contained in the signal. Implicit in this statement is the assumption that the modulation envelope, which can become severely distorted in highly dispersive media, retains its shape.

II. THEORY

Because the ionosphere is a dispersive medium, a quasi-monochromatic signal, i.e., a pulse of radio energy with most of its spectral components centered about an angular frequency, ω, travels through the ionosphere with a group velocity different from the phase velocity associated with the angular frequency, ω. The effective group path length P' is given by

$$P' = \int_0^s \mu' \, dL \, , \tag{1}$$

where the group refractive index

$$\mu' = \frac{d}{d\omega} (\omega\mu) = \mu + \omega \frac{d\mu}{d\omega} \, . \tag{2}$$

Under conditions in which the magneto-ionic splitting of the rays can be ignored,

$$\mu^2 = 1 - X \,, \tag{3}$$

where

$$X = \omega_N^2/\omega^2 = Ne^2/\epsilon_0 m\omega^2$$

and

N = number density of free electrons,
e = charge on an electron,
ϵ_0 = electric permittivity of free space, and
m = mass of an electron.

At VHF, X will be small compared with unity, and it is appropriate to take

$$\mu \approx 1 - \tfrac{1}{2} X \,. \tag{4}$$

The excess $\Delta\ell'$ of the group path length over the free space propagation path length is given by

$$\Delta\ell' = \int (\mu' - 1)\, d\ell \approx \int (1 - \mu)\, d\ell \approx \tfrac{1}{2} \int_0^s X\, d\ell \,. \tag{5}$$

The group-path delay is, of course, simply

$$\Delta T = (\Delta\ell'/c) \approx \frac{e^2}{2c\epsilon_0 m} \cdot \frac{1}{\omega^2} \int_0^s N\, d\ell = \frac{5 \times 10^{-6}}{\omega^2} \int_0^s N\, d\ell \,. \tag{6}$$

From (6), the integrated electron density along the propagation path is

$$\int_0^s N\, d\ell \approx 2 \times 10^5 \omega^2 (\Delta T) \,. \quad \text{(MKS)} \tag{7}$$

For a flat earth, assuming the ray path does not deviate appreciably from a straight line, on changing the variable of integration we have, to a first order,

$$\int_0^6 N \, d\ell = \int N \sec i \, dh \approx \sec i_0 \int N \, dh \, . \qquad (8)$$

With reference to Fig. 1, i is the local zenith angle, while i_0 is the zenith angle at the surface. The integral $\int N \, dh$ is the columnar electron content, which is equivalent to the total number of electrons in a column of unit base extending from the ground to the satellite.

An explanation of the approximation used in (8) is in order. From Snell's law,

$$\mu_0 \sin i_0 = \mu \sin i \qquad (9)$$

and, from (3), on taking $\mu_0 = 1$, we have

$$\sec i = \frac{\mu}{\sqrt{\mu^2 - \sin^2 i_0}} = \frac{\mu \sec i_0}{\sqrt{1 - X \sec^2 i_0}} \, . \qquad (10)$$

Substituting (4) in (10) and retaining only the first-order term in the expansion of the radical,

$$\sec i \approx \sec i_0 \left[1 - \tfrac{1}{2} X \left(1 - \sec^2 i_0 \right) - \tfrac{1}{4} X^2 \sec^2 i_0 \right] . \qquad (11)$$

By restricting i_0 to moderately small values, the second and third terms inside the bracket are negligibly small compared to unity. (Note also that $X \ll 1$.)

The group time delay cannot be determined without a knowledge of the propagation time over the optical path. However, the differential group time delay, Δt_g, between two quasi-monochromatic signals of

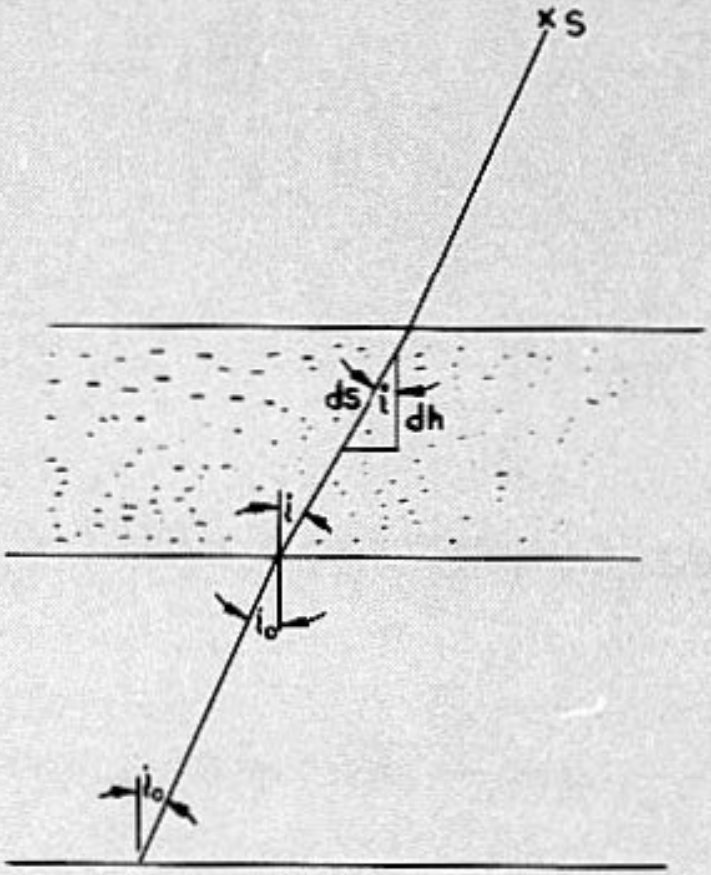

Fig. 1 Trans-ionspheric propagation of quasi-monochromatic signals (slab ionsphere).

frequencies ω_1 and ω_2 can be measured. In terms of the differential group time delay, the columnar electron content to the first order, from (7) and (8), is given by

$$\int N\,dh \approx \frac{2 \times 10^5 \omega_1^2 \omega_2^2 \Delta t_g \cos i_o}{\left(\omega_2^2 - \omega_1^2\right)} \cdot \text{(MKS)} \qquad (12)$$

Use of numerical techniques to include the effects of magneto-ionic splitting, or of more complicated geometries, e.g., spherical stratification, and to take into account contributions from second-order terms, although entirely feasible, is unwarranted for present purposes.

III. INSTRUMENTATION

Satellite

The primary mission of the Vela satellite experiment is to detect a nuclear detonation. This is accomplished in part by sensing the EMP or radioflash emission associated with the explosion. For present purposes, it is sufficient to state that the Vela IV satellite provided surveillance of a number of discrete channels in the dekametric wavelength band. Additional circuitry was incorporated into the satellite payload to provide a very coarse measurement of the time interval between the arrival of two signals having significant, i.e., detectable, energy in the passbands of the receivers.

Figure 2 shows a block diagram of the satellite instrumentation used in the dispersion experiment. Video outputs of each receiver are fed to trigger generators which produce trigger pulses of uniform amplitude and duration anytime the receiver outputs exceed preset levels. Because the group delay time is inversely proportional to the square of the carrier frequency, the trigger from the high-frequency receiver is used to open a gate which is subsequently closed by a trigger from the low-frequency receiver. The time interval between the two signals is proportional to the number of clock pulses from the 262-kHz spacecraft clock that pass through the gate to the counter. Counter states are telemetered to the tracking stations.

Receivers used in the dispersion measurement are simple TRF (tuned radio frequency) receivers with three RF stages, each with a gain of 20 dB, followed by a simple diode detector and a video output stage. The bandwidth of each receiver is roughly 1/30 of the center frequency. Nominal sensitivity is -90 dBm and the dynamic range is about 40 dB.

The receivers are fed from several whip antennas, spaced at 60-degree intervals around the spacecraft and located slightly off the equator. Antennas are phased to produce circularly polarized radiation patterns. The spacecraft orientation in orbit is such that the whip antennas are normal to the radius vector from earth to the satellite. Measurements on a boiler plate model indicated a probable sensitivity of roughly 4 microvolts/meter, which is consistent with the calculated

free-space estimate, assuming unity antenna gain, a 3-dB antenna coupling loss, and a receiver sensitivity of -90 dBm.

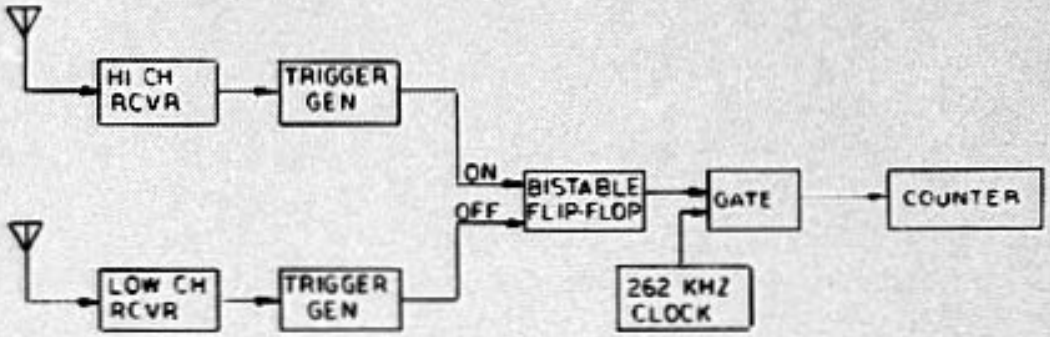

Fig. 2 Receiver configuration for dispersion measurement.

Transmitter

The transmitters used for dispersion measurements belong to a family of spark-gap transmitters developed by Stanford Research Institute (SRI) under ARPA sponsorship.[12] Figure 3 shows a schematic diagram of the transmitter which consisted, essentially, of a coaxial capacitor and a gap-type switch. With half-wave elements directly attached, this transmitter served as the driven element in a yagi array (Fig. 4).

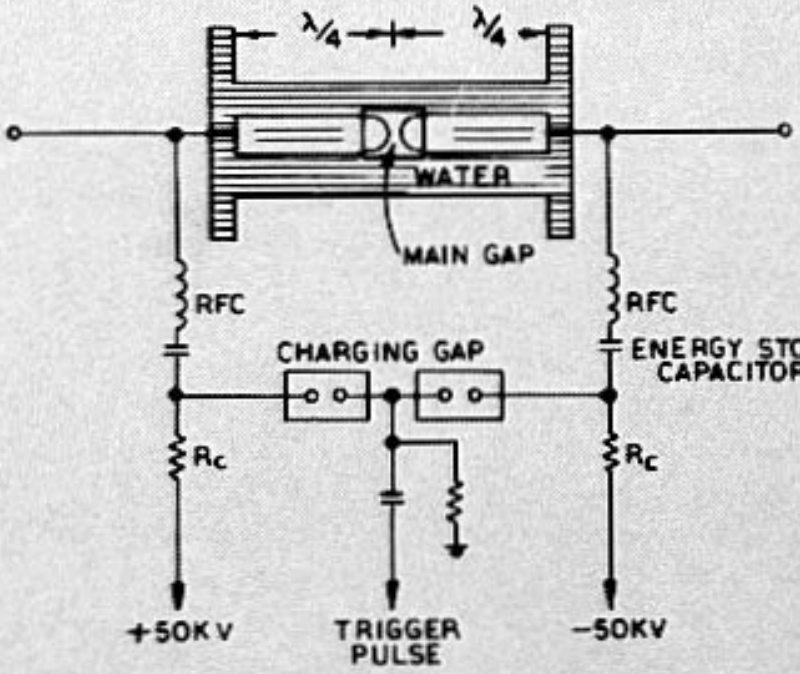

Fig. 3
Schematic diagram of the spark-gap transmitter.

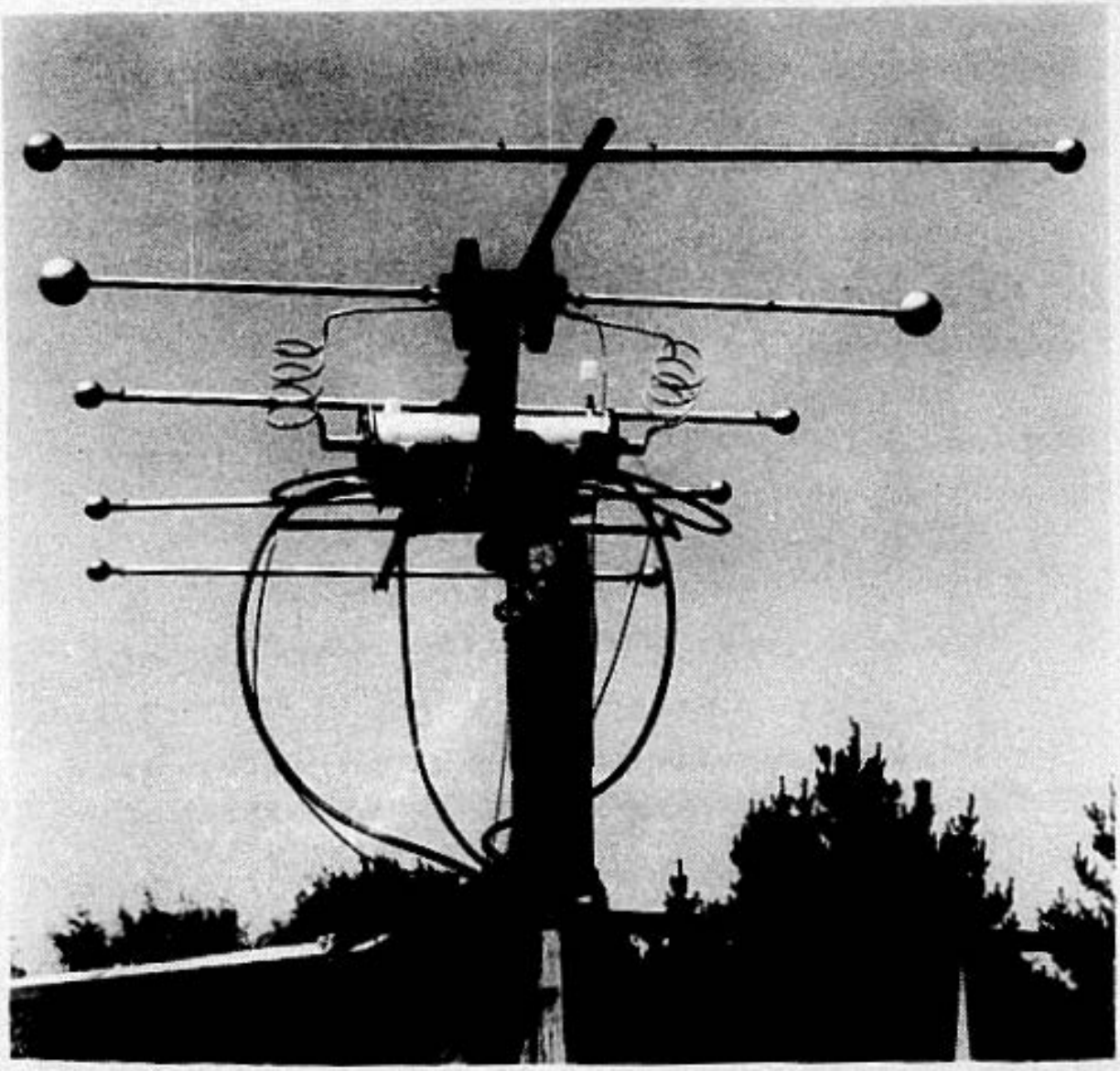

Fig. 4 Spark-gap transmitter antenna array.

Some of the features of this novel design warrant special mention here. By using a tap water dielectric with a dielectric constant of 80, the volume of the capacitor, and therefore the lead inductance, was minimized and a high self-resonant frequency was achieved. Impulse charging, requiring auxiliary spark gaps, was necessary because of the high conductivity of the water. Inconveniences resulting from this complication are mitigated by some additional advantages. These are the immediate self-healing properties of the water when flashover occurs, and the ease of cooling at high power levels and at high pulse repetition rates, simply by changing the water continuously. Safing procedures are simplified since dangerous charges cannot be retained in the presence of a lossy dielectric.

When the central gap fires, a quasi-monochromatic oscillatory discharge is developed. Because the spark-gap resistance decreases with time during the initial portion of the RF pulse, the pulse generated has a rise time of several RF cycles. Typically, the overall pulse envelope, as shown in Fig. 5, appears to be fairly smooth and pseudo-Gaussian. Meaning of the terms quasi-monochromatic and pseudo-Gaussian should be evident from an examination of Fig. 5.

The substitution method was used to measure transmitter pulse power in the far field region. By replacing the pulsed element in the yagi array with a CW source of known strength and comparing envelope amplitudes, the nominal effective radiated power was found to be 10 MW at the frequencies of interest. The peak power produced by the transmitter was estimated to be 1.6 MW.

The transmitting antennas were five-element, horizontally polarized arrays with gains of roughly 8 dB and beamwidths of 25 degrees. Tracking was facilitated by making the antennas steerable.

Completing the description of the transmitting equipment, the overall turn-on jitter was from 3 to 5 nsec, pulse delay was continuously adjustable between channels, and the pulse repetition rate was continuously adjustable from 0 to 30 pulses per second.

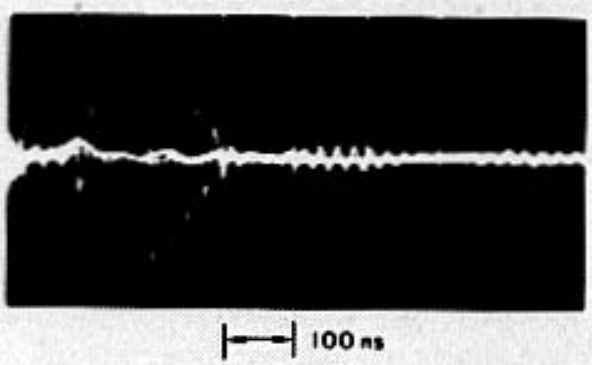

(a) PULSE SHAPE RADIATED BY THE TOWER TRANSMITTER

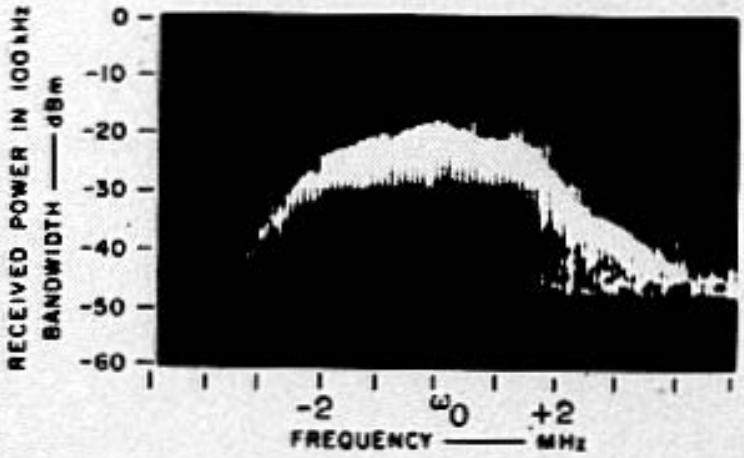

(b) SPECTRUM OF THE TOWER TRANSMITTER

Fig. 5 Typical pulse envelope.

IV. OBSERVATIONAL METHOD

The observations reported here cover the period from October 6 to October 15, 1967. It should be clearly understood that the measurements of total electron content represent an *ad hoc* test. The fact that the electron content was inferred from the observation should be regarded as a dividend from a test specifically designed to calibrate the satellite surveillance system and to verify that dispersion could indeed be significant under certain conditions. That dispersion was a factor to be considered in the design of the Vela system was considered early in the planning phase of the satellite program.[13]

Initial tests were conducted during the latter part of July and the first part of August 1967. During these first tests, certain operational difficulties became apparent. After some remedial work on the transmitting equipment, tests were resumed during the first two weeks of October 1967, when the data reported here were acquired. Preoccupation of the involved personnel with other matters, together with problems concerned with classification difficulties connected with the data reported here, delayed publication of the data analysis until now, although raw dispersion data *per se* have been published elsewhere.*

Figure 6 shows a comparison of the electron content measured simultaneously over three distinct paths on a particular day, October 15, 1967. Calculations are based on Eq. (12). Data points denoted paths 1, 2 were obtained from differential delay measurements made at two different frequencies; a different set of frequencies was used to obtain the data points denoted paths 2, 3. It should be noted that the ordinate scale is logarithmic, so that the agreement between corresponding data points at small zenith angles is roughly comparable to the agreement between data points at large zenith angles.

*R. E. Spalding, Sandia Laboratories, U. S. Technical Paper presented at the Eighth Meeting of the United States-United Kingdom Joint Working Group 16, 31 October-1,2 November 1967.

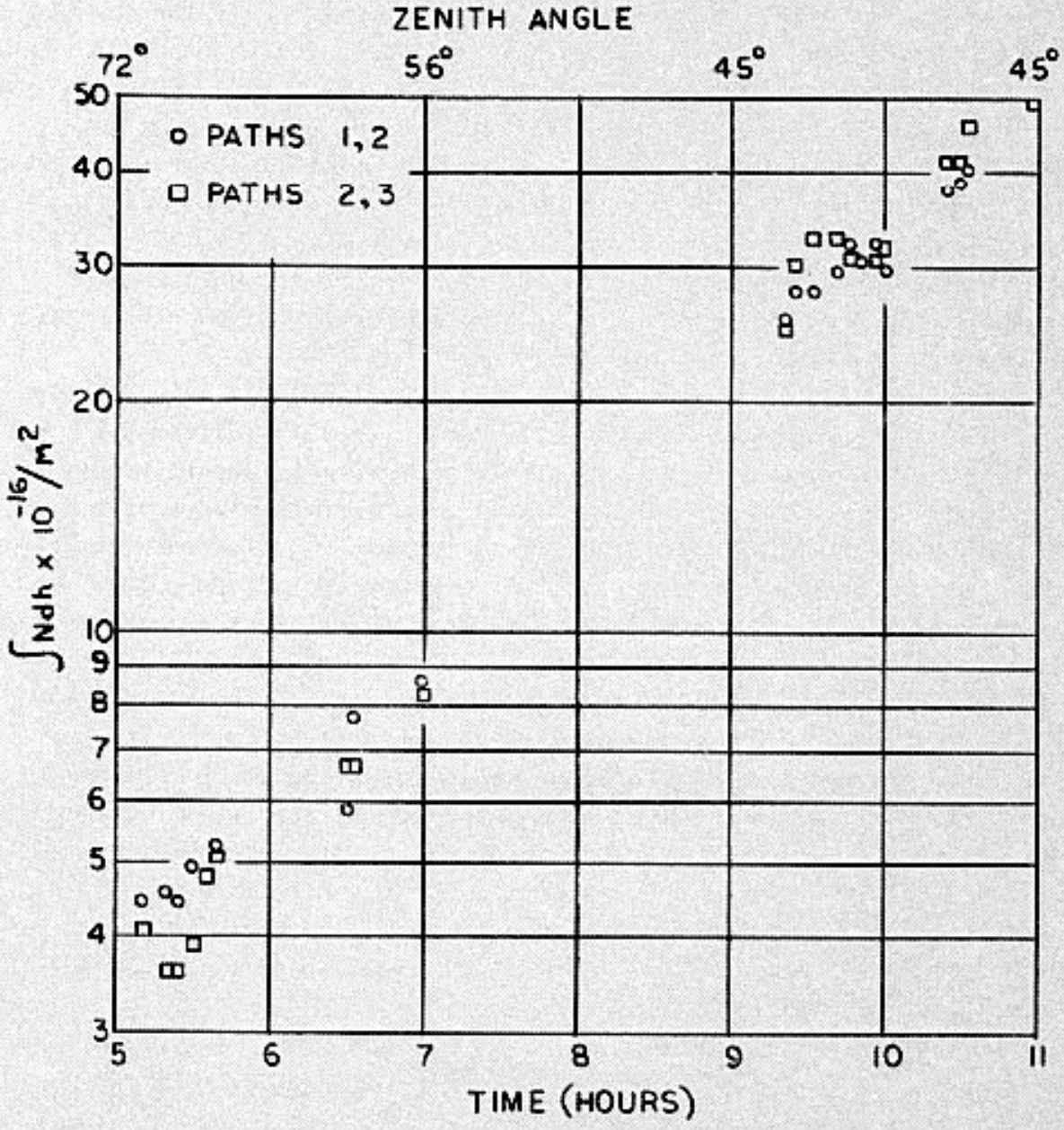

Fig. 6 Slab ionosphere columnar electron content measured simultaneously over several propagation paths.

Because of the possibility of modification in the modulation envelope resulting from pulse dispersion, it is difficult to specify a comparative error ε_i for this experiment. However, provision was made for delayed trigger of the signal sources. Accordingly, errors involved in measuring differential group time delays should be considerably less than the 3.8-μsec time interval between clock pulses (see Fig. 2). An inspection of the spread of data points indicated in Fig. 6 seems to indicate that a value of $\pm 2 \times 10^{16}$ electrons m^{-2} is a reasonable estimate for the accuracy in measurement. This value is consistent with transmitter jitter, as well as the frequencies and bandwidths associated with the receiving equipment and the gross assumption of a slab ionosphere.

Figure 6 shows data acquired during a typical satellite pass lasting 6 hours, although most passes were of shorter duration. By maintaining telephonic communication between the transmitter site at SRI and the Satellite Tracking Center at Sunnyvale, California, definite correlation between transmission and reception of the pulses was established. When the transmitters were turned on and the antennas oriented in the direction of the satellite, pulses were detected by the satellite. In general, triggering was marginal, requiring low noise conditions and favorable satellite look angles for the tests. However, even under favorable conditions, triggering was not always achieved. This was most likely caused by transmitter behavior, particularly a tendency to drift off frequency. As techniques improved, more reliable triggering was accomplished. At times, of course, solar storms occurred, and the background noise levels exceeded signal levels from the transmitters, causing occasional interruptions in the acquisition of data.

V. PRESENTATION OF DATA

Total electron-content data typically take the form of a cyclical presentation (total electron content versus time by days), a mode of presentation that tends to emphasize the diurnal variation in total electron content. This type of data presentation is generally satisfactory because gross changes in electron density with time are not rapid, but occur slowly. For present purposes, the data displayed in Figs. 7 and 8 have been superimposed on an hourly plot to emphasize

rapid changes (seconds to minutes) in electron density, resulting possibly from solar flares or SID (Sudden Ionospheric Disturbance). Figure 7 shows the buildup in total free electron content with time as a result of the absorption of ultraviolet or x-ray photons from the sun.

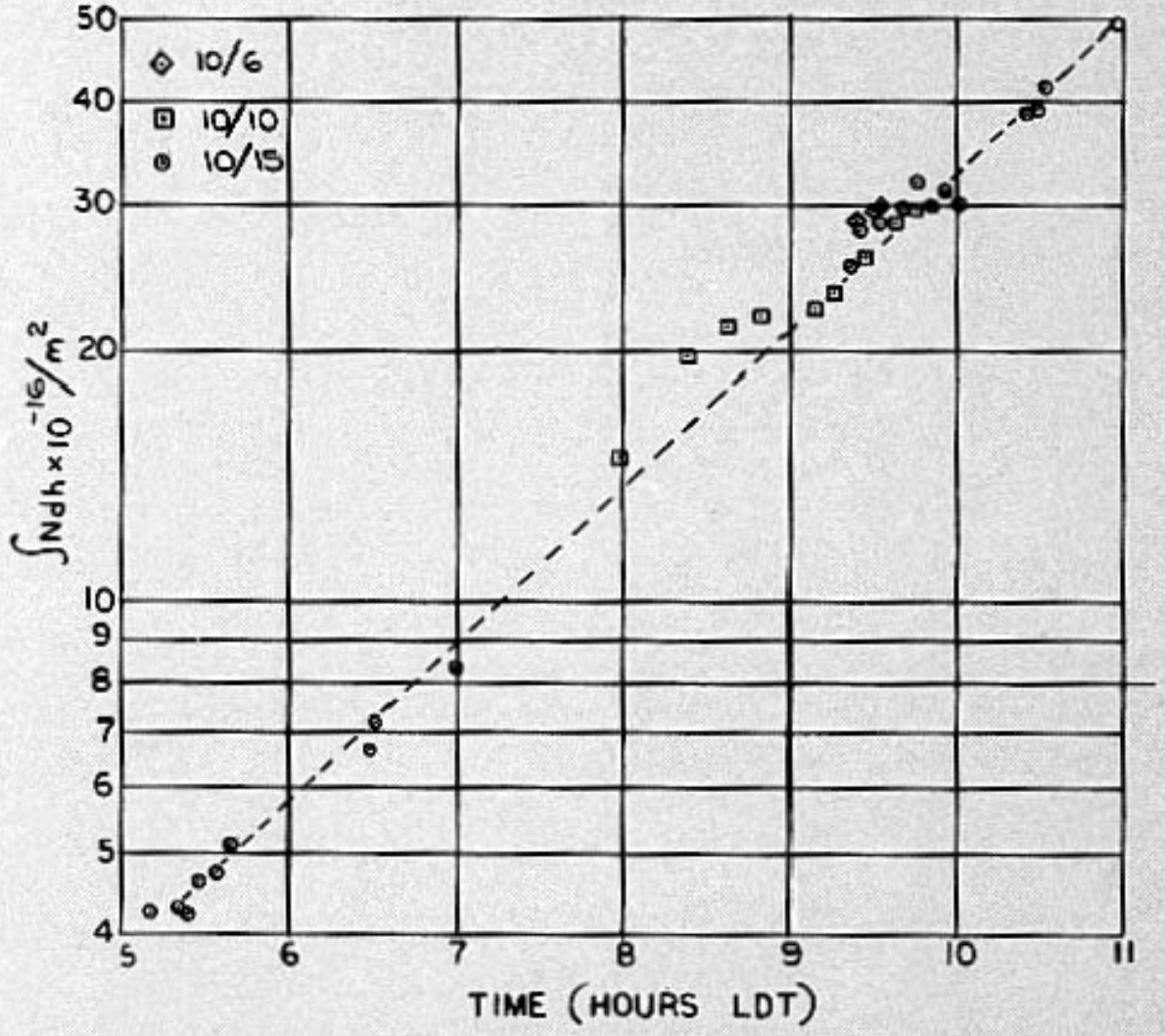

Fig. 7 Slab ionosphere columnar electron content versus time (local daylight), October 1967.

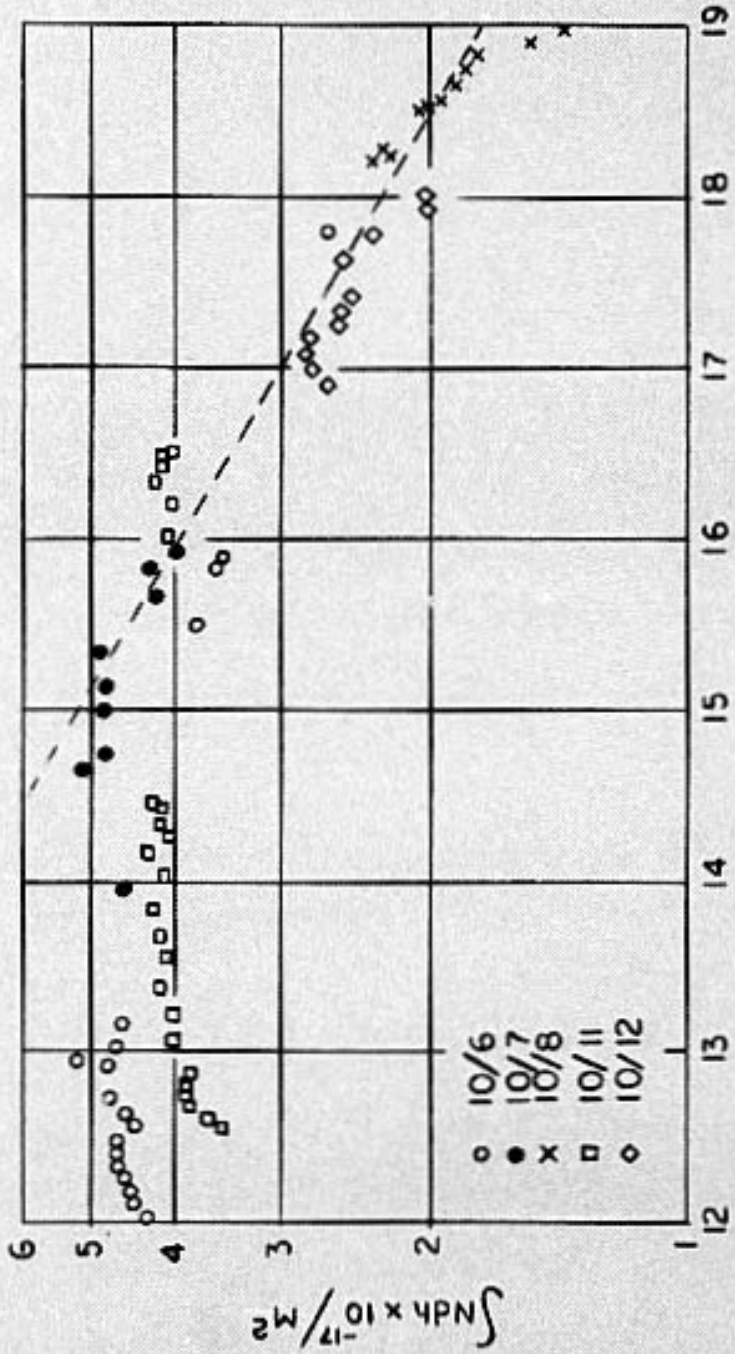

Fig. 8 Slab ionosphere columnar electron content versus time, October 1967.

Absolute values for the total electron content for three separate passes in October 1967 were calculated from Eq. (12), using the maximum measured differential group delay times. Fortunately, in most instances, the zenith angles are small, so that the local daylight time corresponding to each data point, although applicable only to the transmitter site, can also be considered to be the local mean time at the intersection of the propagation path with the slab ionosphere.

Even though the data points are few in number, measurements on the three days indicated show the diurnal variation characteristic of integrated electron density measurements. In general, the daytime electron content is about an order-of-magnitude greater than the nighttime content. The absolute values given do not deviate significantly from those values generally assumed for the ionosphere at the indicated times. For example, on the basis of Doppler shift data, de Mendonca reported nominal values from 4 to 5 $\times$ 10^{17} at noon.[14] Furthermore, according to studies by Lawrence et al., covering the period from September 1958 through December 1959, the usual total electron content changed from roughly 8 $\times$ $10^{16}/m^2$ to 8 $\times$ $10^{17}/m^2$ diurnally.[15] These studies are cited here simply to lend credence to the values given in Fig. 7. Unfortunately, corroborating data for the dates of interest from independent sources and obtained by Faraday rotation or Doppler shift measurements, are unavailable. (Admittedly, total electron content can vary an order of magnitude in either direction, depending on the season and the position in the sunspot cycle. However, the values cited here do correspond roughly with respect to geographical position, season, and sunspot cycle.)

Figure 8 shows the free electron morphology during the period following attainment of peak ionization, nominally 1200 LDT. The graph shows data for five passes during the period from October 6 through October 12, 1967. Note that the electron content remains essentially constant from 1200 to 1600. During this period, a state of equilibrium exists in the region where most of the electrons are located, the rate of electron reproduction balancing the rate of loss. Decay of electrons increases substantially after 1600.

VI. INTERPRETATION OF DATA

Although the data presented in Figs. 7 and 8 are insufficient to warrant extensive analysis, they do merit some discussion, at least for tutorial purposes. As stated above, it should be noted that the primary objective of the experiment was to determine a range of group delays applicable to certain frequency bands of interest. A secondary objective of the study reported here was to determine electron morphology and associated ion chemistry as a function of time. First let us note that it is reasonable to restrict the analysis which follows to the thermosphere, which for present purposes we consider to be the F region of the ionosphere. Contributions to the total electron content from electrons in the exosphere, the region above 380 km, and from electrons in the E and D regions, which extend downwards from 120 km, can be neglected since electron densities in these regions, typically, run from one to two orders of magnitude less than electron densities in the F region. Therefore, it appears justifiable to take as our model a slab of electrons in which the ion chemistry conforms to that generally appropriate for the F region.[16,17] Continuing along this line, we assume that the major neutral constituents are O and N_2 with some O_2. The ions produced by photoionization are O^+, N_2^+, and O_2^+, with N_2^+ and O^+ concentrations roughly equal at 110 km, with O^+ predominating above this altitude. Because O_2 is a minor constituent of this part of the atmosphere, most of the O_2 ions are produced by transfer reactions, i.e., charge exchange or ion atom interchange. The principal loss mechanism for electrons is assumed to be dissociative recombination of the type

$$NO^+ + e \rightarrow N^* + O^* \ , \qquad (13)$$

where the asterisk denotes that the atoms may be left in excited states. The nitric oxide is formed by the two reactions

$$O^+ + N_2 \rightarrow NO^+ + N \qquad (14)$$

and

$$N_2^+ + O \rightarrow NO^+ + N \ . \qquad (15)$$

The time derivative of electron density n at a height h above the earth's surface is given by the equation of continuity

$$\frac{\partial n}{\partial t} = q - \ell(n) - \mathrm{div}(nv) \ , \tag{16}$$

where q is the rate of production of electrons by ionizing radiation and ℓ is the loss rate of electrons. The divergence term is a generalized movement term which includes the effects of diffusion and of mass motion produced by electromagnetic and tidal forces. In order to simplify the analysis, it can be assumed that horizontal gradients can be neglected and that, for present purposes, only the vertical derivatives are important. Integrating both sides of (16) with respect to h and taking $n \approx 0$ at both low and high altitudes, we obtain

$$\frac{d}{dt} \int_0^\infty n \, dh \approx \int_0^\infty q \, dh - \int_0^\infty \ell \, dh \ . \tag{17}$$

The physical meaning here is that the integrated number of electrons remains unchanged, although they may move vertically.

It is generally accepted that the dominant ion species in the upper F region is O^+. At sunrise, the O^+ ions do not recombine with electrons directly except by a very slow radiative process. Instead, they recombine with electrons through the two-step process

$$O^+ + N_2 \rightarrow NO^+ + N \ , \tag{14}$$

$$NO^+ + e \rightarrow N + O \ . \tag{13}$$

Reaction (13) proceeds so rapidly compared with reaction (14) that the overall loss rate is determined by the reaction rate of (14). In this case, the loss term in the continuity equation is simply proportional to the number of electrons present, and the equation of continuity can be written

$$\frac{dN}{dt} + \beta N = Q(t) \ , \tag{18}$$

a simplified equation of continuity in which Q and βN are the integrated production and loss terms, respectively, with dimensions m^{-2} sec^{-1}, and β is an effective attachment coefficient.

In reality, Eq. (18) is applicable only for large solar zenith angles. At later times, as the solar zenith angle decreases and the ionizing radiation reaches the lower regions, in particular the F_1 region (nominally 120-180 km), the loss term in the continuity equation takes the form

$$L = \alpha N^2 . \qquad (19)$$

The most likely diatomic ion-atom interchanges are

$$N_2^+ + O \rightarrow NO^+ + N$$

and

$$O_2^+ + N \rightarrow NO^+ + O .$$

Again, electrons produced in the ionizing process are removed by dissociative recombination, reaction (13).

Unfortunately, measurements of the total electron content do not permit differentiation between the particular ion species involved in the reactions. Only information on the gross behavior of the ionosphere can be obtained. However, by assuming simple models of the ionosphere and by conducting measurements during those times that one of the loss processes described above is dominant, inferences can be drawn on possible sources for the production of electrons.[18-20] Furthermore, by assuming an appropriate profile for the electron density, an equivalent "slab thickness," defined as the ratio of the total electron content to the maximum electron concentration, can be estimated. Because the slab thickness is related to the "plasma temperature" of the ionosphere, measurements of the time rate of change of slab thickness provide a potential source of information on sudden time variations in the temperature of the thermosphere. In the discussion which follows, special emphasis will be placed on the unique possibilities of application of the Vela to these types of studies.

With reference to Fig. 7, clearly the data points for October 15 show a reasonable fit to a straight line. The corresponding empirical relationship for the buildup in electron density is given by

$$N = N_0 e^{\gamma t} , \qquad (20)$$

where $N_0 = 4 \times 10^{16}$ electrons m^{-2} and $\gamma = 1.2 \times 10^{-4}$ sec^{-1}. Furthermore, data points acquired during the buildup between 0900 and 1100 LDT on October 6 and October 10 show fair agreement with the same plot. Obviously, neither of the forms given above for the loss terms are applicable for the entire period of interest covered in Fig. 7. Therefore, it is quite remarkable that such a complex set of ionization phenomena could be represented by the simple empirical form given by Eq. (20). However, the time dependence shown in Fig. 7 is typical of the temporal variation in total electron content determined by a variety of experimental techniques.

In view of the close fit of the data points to the empirical curve of Fig. 7, the apparent marked increase in electron content between 0800 and 0900 LDT on October 10 is particularly interesting. At the time of interest, the spacecraft had just emerged from the magneto shield into the solar wind. For heights above 160 km during the daytime, effective absorption cross sections for ionizing electrons in the 10^2 and 10^3 eV range are one or two orders of magnitude greater than those expected for solar ultraviolet radiation.[21] Now the Vela satellites are equipped to provide information on ionizing particle fluxes. However, electron detectors on the particular satellite used in this experiment failed to indicate any unusual particle fluxes at the time of interest.* It should be noted that no solar x-ray flares were reported on October 10 (see Appendix A). Except for a few minor subflares occurring between 0700 and 1000 LDT,[22] the only unusual chromospheric activity reported was some active limb prominence regions between 0642 and 1222 LDT (1814-1830 UT Sacramento Peak Observatory).[23] However, Appendix A (the Abbreviated Calendar Record) lists October 10 as "one of five most magnetically disturbed days." At the time of the marked deviation of the total electron content from the empirical curve

*S. J. Bame, LASL, personal communication.

of Fig. 7, the geomagnetic activity index K_p increased to 5. That is, the marked deviation (if it is statistically significant) may very well be related to the magnetic activity.

With reference now to Fig. 8, the steady state value of the total electron content between 1200 and 1600 appears to be roughly 4×10^{17} electrons m^{-2}. If an equivalent slab ionosphere thickness of 260 km, extending from 120 to 380 km, is assumed,[18] the average electron density is 1.5×10^6 electrons cm^{-3}. Moreover, in order to simplify the model further, we also assume that this electron density is appropriate to the transition region where molecular ions just begin to predominate over atomic ions and, in particular, that the loss rate is determined by the specific reaction

$$N_2^+ + O \rightarrow NO^+ + N \ , \qquad (15)$$

which has a laboratory rate coefficient[24] of

$$\alpha = 2.5 \times 10^{-10} \ cm^3 \ sec^{-1} \ .$$

In the steady state $(\partial n/\partial t) \approx 0$, the loss term for a reaction involving a molecular ion is of the form αn_e^2, and the continuity equation (16) can therefore be written

$$q_0\left[N_2^+\right] \approx \alpha n_e^2 \approx 5.6 \times 10^2 \ cm^{-3} \ sec^{-1} \ . \qquad (21)$$

The corresponding maximum integrated production rate $Q_0\left[N_2^+\right]$ is $1.4 \times 10^{14} \ m^{-2} \ sec^{-1}$.

By extrapolating total electron content measurements made at sunrise when the rate of production of ion-electron pairs in the ionosphere is much larger than the rate of loss of electrons, Garriott and Smith[19] have calculated the integrated production rate for an overhead sun.* From observations of Syncom III, autumnal transmissions

*In the case of a Vela experiment, the incident photon flux can be measured directly and the integrated production rate for an overhead sun estimated on the basis of an assumed ionizing efficiency.

at Hawaii, substantiated by independent measurements at Stanford, the integrated electron production rate was calculated to be 1.4 (±0.3) × 10^{14} m^{-2} sec^{-1}, with little variation reported from day to day. The calculation assumed a single-constituent, atomic oxygen atmosphere. The loss rate, of course, was of the form βN.

All we are implying here is that, at equilibrium, the rate of electron loss resulting from dissociative recombination (αN^2 type loss) is probably roughly equal to the electron loss resulting from an ion-atom interchange reaction (βN type loss).

With further reference to Fig. 8, between 1600 and 1800 the total electron content decays (denoting 1600 LDT as zero time) approximately as the empirical relationship

$$\int N \, dh = 4 \times 10^{17} \exp(-8 \times 10^{-5} t) \, . \qquad (22)$$

During this two-hour period, the electrons decrease with a half life of about 8.65×10^3 sec. This progressive decrease in electron density is the result of the decrease in effectiveness of the sun's radiation in maintaining ionization as night approaches. At 1600 LDT, there should be little change in the electron density in the F_2 region. Moreover, we have disregarded E and D region contributions to the total electron content. Therefore, we must conclude that the observed decrease in total electron content must be the result of dissociative recombination of electrons in the lower F_1 region. Because the ions in this region are predominantly molecular, an αN^2 type loss must occur. A lower limit to the value of α can be obtained by writing the continuity equation in the form

$$\frac{\Delta n}{\Delta t} \sim \alpha n^2 \, . \qquad (23)$$

Taking Δt equal to the half life $t_{1/2}$, we obtain

$$\alpha \sim \frac{1}{2 n t_{1/2}} \, . \qquad (24)$$

Assuming a standard profile, it is reasonable to choose an electron density about an order of magnitude less than that used for the peak electron density in the F_2 region. Accordingly, the rate constant given by (24) for an electron density of the order of 10^5 cm^{-3} is roughly 5×10^{-10}. The most likely reactions are

$$N_2^+ + O_2 \rightarrow N_2 + O_2^+$$

and

$$N_2^+ + O \rightarrow N + NO^+ .$$

Examination of Fig. 8 shows considerable scatter of data points about the assumed equilibrium value. Although the apparent scatter may be attributable either to experimental error or to fluctuations in the ionizing radiation, an alternative, but highly intriguing, interpretation can be given.* First, it should be noted that most of the scatter occurs at noon and during the period between 1200 and 1800. Second, most of the ionization occurs at 200 km where the ions are predominantly O^+. Even with the assumption of a two-constituent ionosphere, the principal nitrogen ion reaction could be the simple charge transfer mechanism

$$N_2^+ + O \rightarrow O^+ + N_2 . \qquad (25)$$

In any case, the O^+ formed either by photoionization or charge transfer interacts with nitrogen to form nitric oxide in the ion-atom interchange reaction

$$O^+ + N_2 \rightarrow N + NO^+ .$$

*The authors are indebted to F. P. Hudson for calling their attention to this possibility.

Now, if the N_2 is vibrationally excited, the rate constant for the reaction

$$O^+ + N_2(T_v) \rightarrow N + NO^+ \qquad (26)$$

is increased by a factor of about 20 at a vibrational temperature (T_v) of approximately 3000°K over the rate constant for the ground vibrational state N_2.[25,26] Because reaction (26) converts an atomic ion with a low electron recombination coefficient to a molecular ion with a large electron recombination coefficient, any changes in the rate constant of reaction (26) would produce a marked effect on electron density.

Relative again to Appendix A, it should be noted that almost the entire period between October 6 and October 15, 1967, could be characterized as a period of marked magnetic activity. Now, a number of observers have correlated periods of high magnetic activity with changes in total electron content.[15,27,28] However, of particular interest to us in this connection is a suggestion by Schmeltekopf et al.[25] that magnetic storms may affect nitrogen vibrational excitation, thereby changing the reaction rate of (26). Further discussion of possible relationships between sudden geomagnetic commencements and the total ionospheric electron content is beyond the scope of the present paper. However, it very well may be that the Vela satellite could be used to provide additional information on the relationship between magnetic activity and the vibrational temperature of molecular nitrogen in the thermosphere.

Admittedly, the treatment of the data presented here has been superficial. In order to simplify the presentation, some of our assumptions have been very naive. On the other hand the criticism could be leveled that too much has been inferred from a fairly small sample of data. Nevertheless, the twofold objective of the present paper should be kept in mind. First, we have attempted to justify extension of the Vela satellite program to substantially extend our knowledge of temporal variations in the total electron content of the atmosphere. Second, it is hoped that the present paper may serve as an outline for a more comprehensive study if one should be undertaken.

VII. CONCLUSIONS AND RECOMMENDATIONS

The variation of the total electron content of the ionosphere with time has been determined by measurements of differential group delays of signals propagated over an earth-Vela satellite path. Although launched in 1966, the Vela IV satellites used in the experiments are still operational and presumably could be made available for a continuation of the cursory studies reported here. Continued interest by communications engineers in the effects of dispersion on signal propagation over earth-satellite propagation paths is almost sufficient to warrant a more vigorous experimental program.

The experimental technique used here is obviously superior to lunar echo sounding methods in determining the total electron content because of the higher signal-noise ratios obtainable over the short (18 earth radii) propagation path length to the Vela satellite. The advantage of the group velocity technique over the Faraday rotation technique is more subtle. At night, and especially during periods of low electron densities, Faraday fading rates become comparable to satellite spin stabilization rates. Nighttime measurements would be useful in studies of ionization possibly induced by energetic electrons, a mechanism often nentioned as responsible for the maintenance of the F region at night.

In recent years, interest in temporal changes in total electron content has increased with the availability of geostationary satellite beacons. Although the Vela IV satellite is in a nonsynchronous orbit, it is uniquely equipped for total electron content measurements. In addition to the dispersion measurement capability described here, it should be noted that the Vela satellites are equipped with sensors which analyze the ultraviolet flux in the range 120-900 Å. Therefore, it should be feasible to correlate changes in the total electron content with changes in the photon flux responsible for most of the ionization observed. Moreover, the satellite is equipped with electron-proton spectrometers covering a range of energies from 33 keV to 20 eV, a specially useful range of energies in connection with studies of corpuscularly induced F region ionization.

Finally, as the relationship between slab thickness and plasma temperatures becomes better understood, the primary mission of the Vela IV satellites, existing instrumental facilities, can profitably be extended to provide experimental data on high-altitude sources of vibrational energy.

In conjunction with other techniques, it appears that this unique facility can provide information on a variety of transient phenomena connected with the F region of the atmosphere, a very dynamic region of the earth's environment.

REFERENCES

1. O. K. Garriott and R. N. Bracewell, "Satellite studies of the ionization in space by radio," in Advances in Geophysics, H. E. Landsberg and J. van Mieghem, eds., Vol. 8, Academic Press, New York, 1961, pp. 85-133.

2. Johnathan Mass, "Survey of satellite techniques for studying propagation," in Radio Astronomical and Satellite Studies of the Atmosphere, Jules Aarons, ed., North-Holland Publishing Company, Amsterdam, 1963, pp. 256-288.

3. F. G. Smith, "Ionospheric refraction of 81.5 Mc/s radio waves from radio stars," J. Atmospheric Terrest. Phys., 2, 350, 1952.

4. A. H. Taylor and E. O. Hulburt, "Propagation of radio waves over the earth," Phys. Rev., 27, 189, 1926.

5. G. Breit and M. A. Tuve, "Existence of the conducting layer," Phys. Rev., 28, 554, 1926.

6. I. C. Browne, J. V. Evans, J. K. Hargreaves, and W. A. S. Murray, "Radio echoes from the moon," Proc. Phys. Soc. B, 69, 901, 1956.

7. J. V. Evans, "The measurement of the electron content of the ionosphere by the lunar radio echo method," Proc. Phys. Soc. B, 69, 953, 1956.

8. J. V. Evans, "The electron content of the ionosphere," J. Atmospheric Terrest. Phys., 11, 259, 1957.

9. G. J. Aitchison and K. Weekes, "Some deductions of ionospheric information from the observations of emissions from satellite 1957 α2-I," J. Atmospheric Terrest. Phys., 14, 236, 1959.

10. G. J. Aitchison, J. H. Thomson, and K. Weekes, "Some deductions of ionospheric information from the observations of emissions from satellite 1957 α2-II," J. Atmospheric Terrest. Phys., 14, 244, 1959.

11. K. Weekes, "On the interpretation of the Doppler effect from senders in an artificial satellite," J. Atmospheric Terrest. Phys., 12, 335, 1958.

12. L. T. Dolphin and F. E. Frith, Spark Transmitter Techniques for EM Pulse Generation, Stanford Research Institute Report, SRI Project 4548, August 1966.

13. R. D. Jones, W. C. Myre, and F. J. Wymer, Vela III W System, Sandia Laboratories Report SC-DR-66-15, January 1966.

14. Fernando de Mendonca, "Ionospheric electron content and variations measured by Doppler shifts in satellite transmissions," J. Geophys. Res., 67, 2315, 1962.

15. R. S. Lawrence, D. Jane Posakony, O. K. Garriott, and S. C. Hall, "The total electron content of the ionosphere at middle latitudes near the peak of the solar cycle," J. Geophys. Res., 68, 1889, 1963.

16. T. M. Donahue, "Ionospheric composition and reactions," Science, 159, 489, 1968.

17. H. Rishbeth and O. K. Garriott, Introduction to Ionospheric Physics, Academic Press, New York, 1969, pp. 113-125.

18. G. N. Taylor, "Integrated electron production and loss rates in the ionosphere," Planet. Space Sci., 13, 507, 1965.

19. O. K. Garriott and F. L. Smith III, "The rate of production of electrons in the ionosphere," Planet. Space Sci, 13, 839, 1965.

20. F. L. Smith III, "Electron production and loss rates in the F region," J. Geophys. Res., 73, 7385, 1968.

21. John M. Kelso, Radio Ray Propagation in the Ionosphere, McGraw-Hill Book Company, New York, 1964, pp. 66-110.

22. Solar-Geophysical Data, Environmental Science Services Administration, U. S. Department of Commerce, IER-FB-284, 101-110, April 1968.

23. Anne L. Carrigan and Norman J. Oliver, Space Data Bulletin, IV, 105-106, Fourth Quarter, 1967. (Published by Space Physics Laboratory, Air Force Cambridge Research Laboratories, L. G. Hanscom Field, Mass.)

24. F. C. Fehsenfeld, A. L. Schmeltekopf, and E. E. Ferguson, "Correction in the laboratory measurement of the rate constant for $N_2^+ + O_2 \rightarrow N_2 + O_2^+$ at 300° K," Planet. Space Sci., 13, 919, 1965.

25. A. L. Schmeltekopf, F. C. Fehsenfeld, G. I. Gilman, and E. E. Ferguson, "Reaction of atomic oxygen ions with vibrationally excited nitrogen molecules," Planet. Space Sci., 15, 401, 1967.

26. J. C. G. Walker, R. S. Stolarski, and A. F. Nagy, "The vibrational temperature of molecular nitrogen in the thermosphere," Ann. Geophys., 25, 831, 1969.

27. George A. Millman, "The variation of electron content in the ionosphere at a low latitude," in Electron Density Profiles in Ionosphere and Exosphere, Jon Frihagen, ed., North Holland Publishing Co., Amsterdam, 1966, pp. 555-566.

28. M. Mendillo, M. D. Papagiannis, and J. A. Klobuchar, "A seasonal effect in the mid-latitude slab thickness variations during magnetic disturbances," J. Atmosph. Terr. Phys., 31, 1359, 1969.

APPENDIX A

Abbreviated Calendar Records
(October 6, 10, 15, 1967)

APPENDIX A

Abbreviated Calendar Records*
(October 6, 10, 15, 1967)

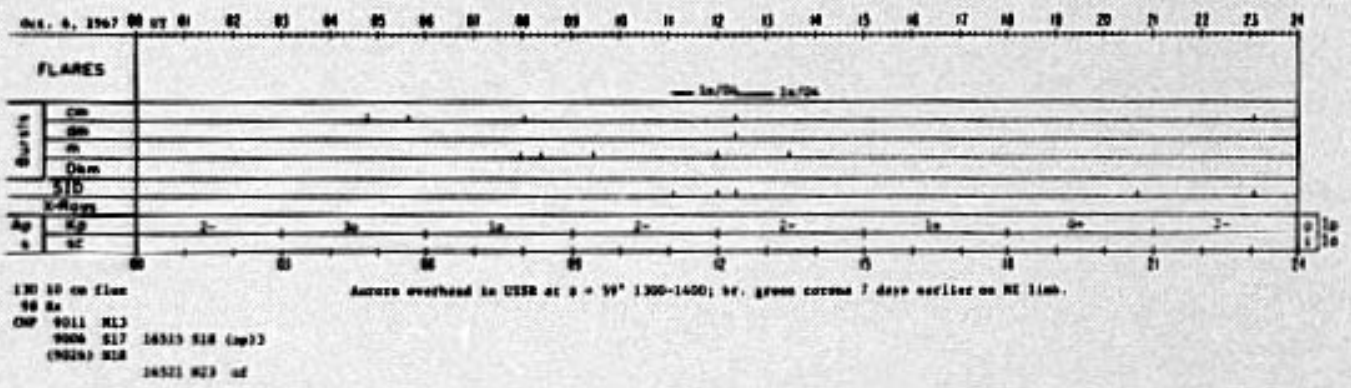

130 10 cm flux
98 Ax
CMP 9011 K13
9006 S17 16515 S18 (sp)3
(9026) S18
16521 N23 sf

Aurora overhead in USSR at φ = 59° 1300-1400; br. green corona 7 days earlier on NE limb.

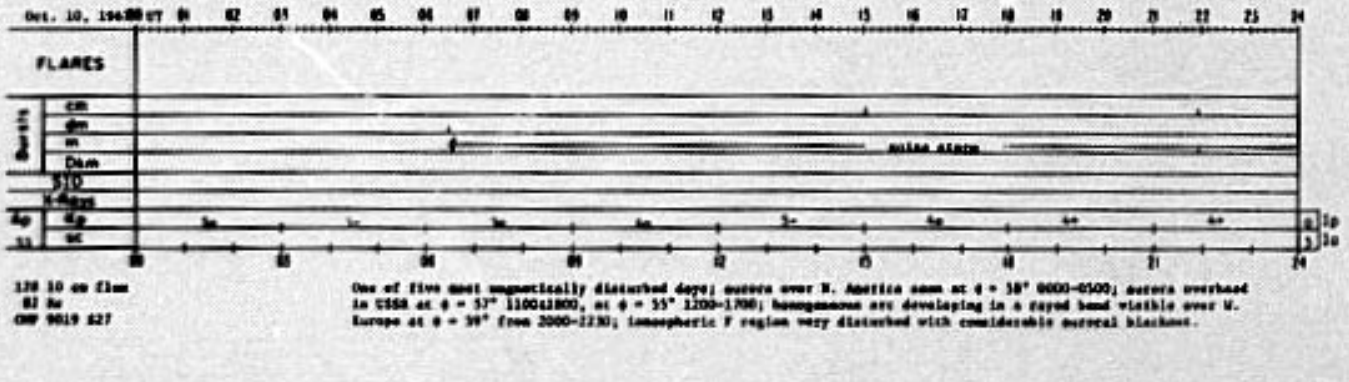

128 10 cm flux
82 Ax
CMP 9019 S27

One of five most magnetically disturbed days; aurora over N. America seen at φ = 58° 0000-0500; aurora overhead in USSR at φ = 57° 1100-1800, at φ = 55° 1200-1700; homogeneous arc developing in a rayed band visible over W. Europe at φ = 59° from 2000-2230; ionospheric F region very disturbed with considerable auroral blackout.

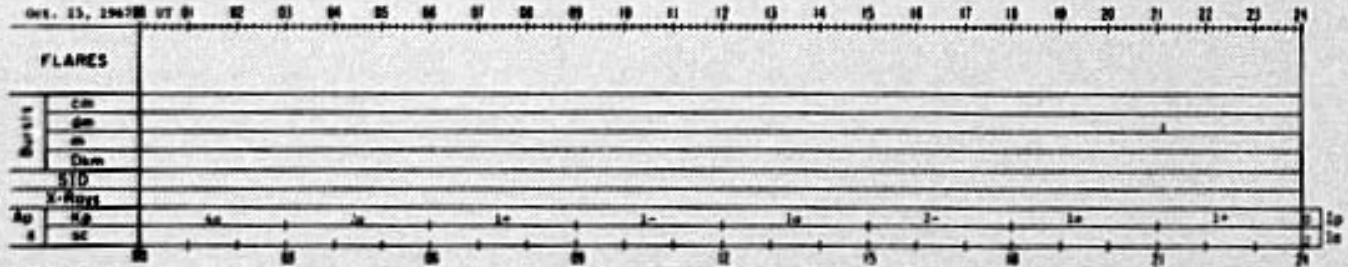

123 10 cm flux
47 Ax
CMP 9020 N18(2)

*J. Virginia Lincoln, Hope I. Leighton, and Dorothy K. Kropp, Abbreviated Calendar Record 1966-1967, 146-148, World Data Center A, Upper Atmosphere Geophysics Report UAC-4, National Academy of Sciences, 2101 Constitution Ave., N.W. Washington, D.C.

Abbreviated Calendar Records
(October 7, 8, 11, 12, 1967)

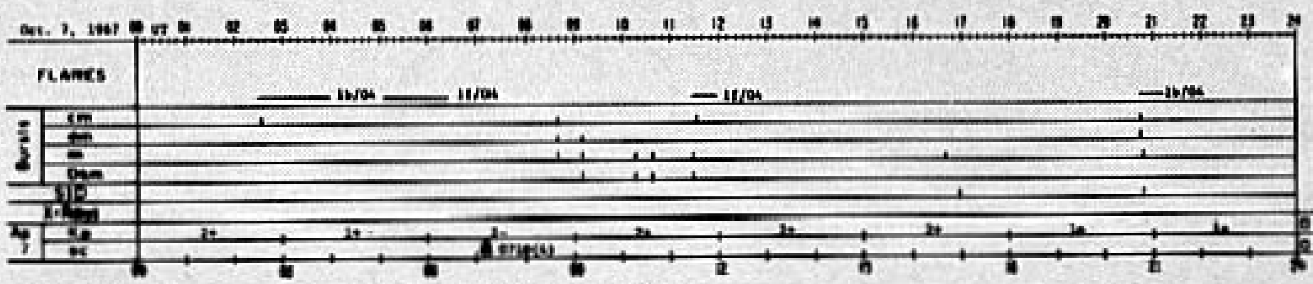

126 10 cm flux
92 Ra
CMP 9012 130(4)

Br. green corona 7 days earlier on EE limb.

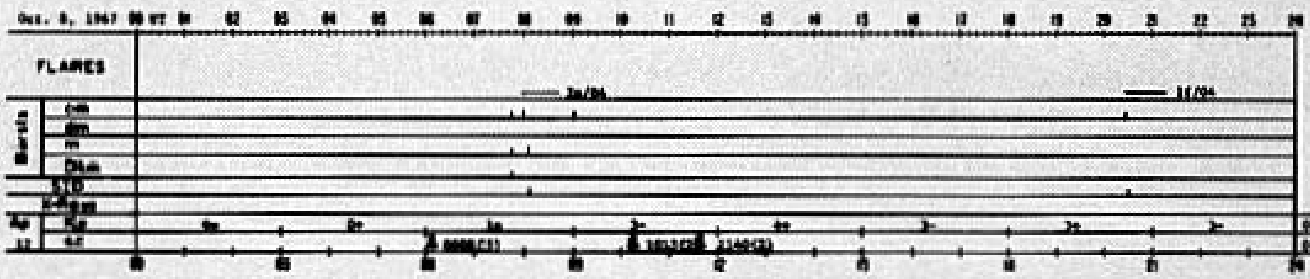

122 10 cm flux
76 Ra
CMP 9013 N12 16519 N11 (Sp)2
9007 N29(3)
9014 N22(2) 16517 S26 (Sp)4

Aurora overhead in USSR at φ = 39° 1300 and at φ = 37° 1400-1800; weak rayed arc visible from 2030-0130 over W. Europe to φ = 38°.

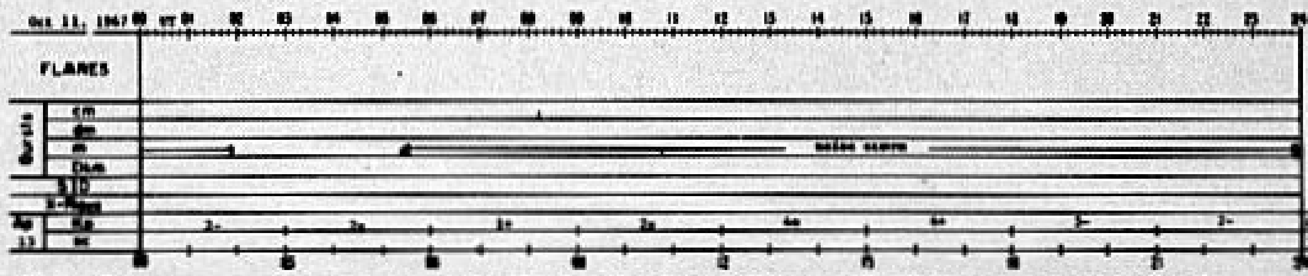

137 10 cm flux
90 Ra
CMP 9018 N18(2) 16524 N15 (Sp)3

Aurora overhead in USSR at φ = 58° 1300 and 1800-1900, at φ = 57° 1600-1700; Ionospheric F region disturbed.

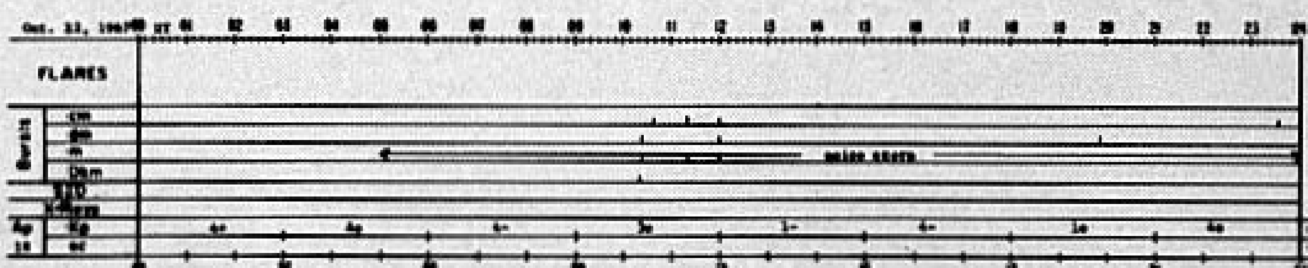

138 10 cm flux
63 Ra

One of five most magnetically disturbed days; Ionospheric F region disturbed in some sectors.

DISTRIBUTION:

Los Alamos Scientific Laboratory (2)
P. O. Box 1663
Los Alamos, New Mexico 87544
Attn: J. H. Malik
R. E. Partridge

D. H. Denton, 100
W. J. Howard, 1000
D. B. Shuster, 1200
W. C. Myre, 1210
T. M. Burford, 1700
C. C. Hudson, 1751
J. W. Kane, 1752
R. S. Claassen, 2600
C. R. Mehl, 5230
C. N. Vittitoe, 5231
F. P. Hudson, 5234
O. M. Stuetzer, 7210
T. L. Pace, 7220
T. B. Cook, Jr., 8000
G. A. Fowler, 9000
B. F. Murphey, 9100
J. R. Banister, 9150
J. H. Scott, 9200
M. L. Kramm, 9210
D. E. Henry, 9211
H. M. Dumas, 9213
R. E. Spalding, 9214
R. D. Jones, 9214
L. E. Anderson, 9217
E. L. Whitlow, 9217
J. C. Eckhart, 9220
H. H. Patterson, 9230
A. Y. Pope, 9300
Library Division, 8232 (5)
Central Files, 3422-1 (15)
L. C. Baldwin, 3412
G. C. McDonald, 3416 (3)